Energetic consequences of nitrite stress in *Desulfovibrio vulgaris* Hildenborough inferred from global transcriptional analysis

Qiang He[1], Katherine H. Huang[2], Zhili He[1], Eric J. Alm[2], Matthew M. Fields[3], Terry C. Hazen[4], Adam P. Arkin[2,5,6], Judy D. Wall[7], and Jizhong Zhou[1*]

[1]Environmental Sciences Division, Oak Ridge National Laboratory, Oak Ridge, Tennessee 37831, USA

[2]Physical Biosciences Division, Lawrence Berkeley National Laboratory, Berkeley, California 94720, USA

[3]Department of Microbiology, Miami University, Oxford, Ohio 45056, USA

[4]Earth Sciences Division, Lawrence Berkeley National Laboratory, Berkeley, California 94720, USA

[5]Department of Bioengineering, University of California, Berkeley, California 94720, USA

[6]Howard Hughes Medical Institute, Berkeley, California 94720, USA

[7]Department of Biochemistry, University of Missouri-Columbia, Columbia, Missouri 65211, USA

*Corresponding author:
Jizhong Zhou
Environmental Sciences Division
Building 1505, Room 390, MS-6038
Oak Ridge National Laboratory
Oak Ridge, TN 37831-6038
Tel: 865-576-7544
Fax: 865-576-8646
e-mail: zhouj@ornl.gov

Running title: Nitrite stress response by *D. vulgaris*

Key words: heavy metal bioremediation, ferric iron uptake regulator, oxidative stress, microarray

Abstract

Many of the proteins that are candidates for bioenergetic pathways involved with sulfate respiration in *Desulfovibrio* spp. have been studied, but complete pathways and overall cell physiology remain to be resolved for many environmentally relevant conditions. In order to understand the metabolism of these microorganisms under adverse environmental conditions for improved bioremediation efforts, *Desulfovibrio vulgaris* Hildenborough was used as a model organism to study stress response to nitrite, an important intermediate in the nitrogen cycle. Physiological studies demonstrated that growth was inhibited by nitrite and that nitrite reduction was observed to be the primary mechanism of detoxification. Global transcriptional profiling with whole-genome microarrays revealed a coordinated cascade of responses to nitrite in pathways of energy metabolism, nitrogen metabolism, oxidative stress response, and iron homeostasis. In agreement with previous observation, nitrite stressed cells showed a decrease in expression of genes encoding sulfate reduction functions in addition to respiratory oxidative phosphorylation and ATPase activity. Consequently, the stressed cells had a decrease in expression of ATP-dependent amino acid transporters and of proteins involved in translation. Nitrite detoxification also appeared to shift the flow of reducing equivalents from oxidative phosphorylation to nitrite reduction. Increased demand for iron, resulting from these regulatory events and the chemical oxidation of available Fe^{2+}, likely contributed to iron depletion and the derepression of the Fur regulon. The regulatory mechanisms during nitrite stress response implicated in this work need to be elucidated by further biochemical studies on *D. vulgaris*.

Introduction

The sulfate-reducing bacteria represent a group of microorganisms characterized by the ability to use sulfate as an electron acceptor in anaerobic respiration (Postgate, 1984). Microbial sulfate reduction by these microorganisms is recognized as a widely distributed process of great ecological importance (Singleton, 1993; Madigan *et al*., 2000). Historical interest in sulfate-reducing bacteria has been focused on their involvement in

biocorrosion of ferrous metals in the petroleum industry and of concrete structures in wastewater collection systems (Hao *et al*., 1996; Little *et al*., 2000). More recent studies (Lovley *et al*., 1993a&b; Lloyd *et al*., 1999; Chardin *et al*., 2002) have documented the ability of a number of sulfate-reducing bacteria to reduce soluble metal oxyanions to insoluble forms, a process of great potential in the bioremediation of toxic heavy metals and radionuclides such as chromium and uranium (Gadd and White, 1993; Valls and de Lorenzo, 2002).

To effectively immobilize heavy metals and radionuclides using sulfate-reducing bacteria, it is important to understand the microbial response to adverse environmental factors common in contaminated subsurface environments. One such factor is the high nitrate concentration of many contaminated sites at the U.S. nuclear weapon complexes managed by the Department of Energy (Riley and Zachara, 1992; NABIR 2003). The presence of nitrate may pose a specific stress to sulfate-reducing bacteria as nitrate was observed to suppress sulfate reduction activity *in situ* (Jenneman *et al*., 1986; Davidova *et al*., 2001). However, it has been suggested that nitrite, an intermediate that transiently accumulates during nitrate reduction (Betlach and Tiedje, 1981; van Rijn *et al*., 1996; Kelso *et al*., 1999), is directly responsible for the inhibition of sulfate reduction activity (Londry and Suflita, 1999; Myhr *et al*., 2002). Therefore, it is important to understand the inhibitory effects of nitrite on the cellular physiology and biochemical capacity of sulfate-reducing bacteria in order to predict their performance for bioremediation.

In this report we used *Desulfovibrio vulgaris* Hildenborough as a model organism to investigate the inhibition of sulfate reduction by nitrite. The microbial stress responses at the transcriptional level were studied with whole-genome microarrays. Our results

indicate that *D. vulgaris* is capable of rapid nitrite reduction and the exposure to nitrite triggers a well coordinated response in pathways of energy metabolism, nitrogen metabolism, oxidative stress response, and iron homeostasis.

Results

Growth inhibition of D. vulgaris by nitrite

The inhibitory effect of nitrite on the growth of *D. vulgaris* was evaluated by adding various concentrations of nitrite to actively growing cultures ($OD_{600\ nm}$ ca. 0.4). No significant growth inhibition was observed with nitrite concentrations below 1 mM as the growth curves overlapped between nitrite-treated cultures and control cultures (Fig. 1). With 2.5 mM nitrite, a slower growth rate was observed. When nitrite concentration increased to 5 mM, the growth of *D. vulgaris* was significantly decreased, and little change in OD was observed over the monitored time (Fig. 1).

Reduction of nitrite by D. vulgaris

To further determine the connection between nitrite and the growth inhibition of *D. vulgaris*, nitrite levels were monitored in the *D. vulgaris* cultures (Fig. 2). Abiotic reduction of nitrite by the medium or sulfide was excluded as nitrite was stable with the presence of 40 mM sulfide in no-cell controls. On the other hand, with initial concentrations lower than 2.5 mM, nitrite decreased rapidly in active *D. vulgaris* cultures, indicating that nitrite was reduced by *D. vulgaris* cells. In contrast, *D. vulgaris* cultures

were unable to reduce 5 mM nitrite, which coincided with nearly complete inhibition of growth as shown in Fig. 1.

Transcriptome analysis of nitrite stress

To study the mechanisms exploited by *D. vulgaris* cells to alleviate the toxicity of nitrite, microarray experiments were carried out to compare global gene expression profiles between nitrite stressed *D. vulgaris* cultures and control cultures without nitrite exposure. In order to achieve an optimal stress response, *D. vulgaris* cells were challenged by a sub-lethal nitrite level (2.5 mM), which effectively inhibited cell growth but still allowed active reduction of nitrite (Fig. 2). Because tolerance to nitrite was suggested to be dependent on the biomass concentration at the time of nitrite addition (Haveman *et al*., 2004), cultures of similar optical densities ($OD_{600\ nm}$ ca. 0.4) were used throughout the study.

Significant changes in gene expression profile occurred within 30 min following nitrite addition and peaked at 60 min with 330 genes being up-regulated and 273 genes down-regulated (Fig. 3) greater than two fold. Subsequently, transcriptional responses rapidly diminished with only 82 genes still up-regulated and 86 genes down-regulated more than two fold 4 hours after nitrite addition (Fig. 3). About the same time, the initial 2.5 mM nitrite concentration dropped below 0.5 mM. The steady decline in transcriptional response subsequent to the changes initially observed mirrored the time course of reduction of nitrite by *D. vulgaris*, showing an apparent correlation between the dynamics of transcriptional response and reduction of nitrite.

To illustrate the gene functions involved in nitrite stress response, genes with altered expression levels after 1h of nitrite exposure were grouped into functional role categories according to The Institute for Genomic Research (TIGR)'s annotation of *D. vulgaris* Hildenborough genome sequence (Peterson *et al*., 2001; Heidelberg *et al*., 2004) as shown in Fig. 4. Notably, a large portion of the highly up-regulated genes belong to cellular roles involved in organic acid oxidation, regulatory functions, and signal transduction, suggesting a shift in energy flow through complex regulatory pathways when *D. vulgaris* cells signal the presence of nitrite. On the other hand, many of the highly down-regulated genes have functions in protein biosynthesis and encode transport and binding proteins, perhaps indicating a slowdown in normal cellular biosynthetic activities when challenged by nitrite stress.

Validation of microarray results

To validate transcriptional results generated by microarray hybridization, real-time RT-PCR analysis was conducted to quantitate the expression levels of eight genes (data not shown). A high degree of correlation was found between results from microarray and RT-PCR (r^2=0.93), as reported in previous studies that used this microarray procedure (Gao *et al*., 2004; Wan *et al*., 2004). The accuracy of this approach in the current study was affirmed.

In addition to real-time RT-PCR analysis, expression differences for gene pairs within the same predicted operon or gene pairs selected at random were compared to determine whether changes observed in microarray experiments were authentic (Gao *et al.*, 2004). Consistent with our expectation (Fig. 5A), genes within the same operon responded more

similarly than did genes randomly selected from the genome. As shown in Fig. 5A, the within-operon pairs had higher probabilities to exhibit much smaller log-ratio differences than gene pairs chosen at random, thus confirming the agreement between microarray results and operon prediction, and the high quality of the expression data. Furthermore, a second operon-based computational method was also used to test the validation of the microarray results through evaluation of the confidence levels of gene expression (Price *et al*., 2005). Consistently, genes identified as confident changers were generally in close agreement with other genes found in the same operon (Fig. 5B). In addition, at the 90 min time point, about half of the genes measured were identified as confident changers. Thus the comparison with operon structure confirmed both the high quality of the expression data, and our ability to identify which data points were most reliable.

Hierarchical clustering analysis of temporal gene expression profile

To understand the various mechanisms involved in nitrite stress response by *D. vulgaris*, a hierarchical clustering analysis was conducted on the transcriptional profile (Fig. 6). Cluster A consists of genes highly induced throughout the duration of the experiment, including the operon encoding the nitrite reductase and several redox-active proteins. Notably, the hybrid cluster protein was highly up-regulated in response to the presence of nitrite, providing more evidence for its suggested role in nitrogen metabolism (van den Berg *et al*., 2000; Wolfe *et al*., 2002). Cluster B represents a group of genes highly induced within 1.5 h of the addition of nitrite but for which the induction diminished or even reversed subsequently. Interestingly, genes included in this cluster encode for ferrous iron transport proteins, suggesting the important role of iron homeostasis in the

initial stress response to nitrite. Cluster C covers a large number of genes repressed during the early response to nitrite that were later restored to expression levels observed in the control cultures. Within Cluster C, genes for ribosomal proteins were particularly in abundance, consistent with prior findings of an early slowdown in protein synthesis (Fig. 4). Cluster D is comprised of genes down-regulated throughout the experiment duration, including genes that have functions in energy metabolism. From the concurrent induction of genes in nitrite reduction (Cluster A) and the repression of genes encoding ATP synthase subunits (Cluster D), we inferred that electron flow was likely shifted from respiratory phosphorylation to the reduction of nitrite.

Genes involved in energy metabolism

Genes having functions in energy metabolism exhibited considerable divergence in their transcriptional response to nitrite (Table 1). In contrast to the severe repression of ATP synthase genes, genes encoding the membrane-bound lactate dehydrogenase (*ldh*) and pyruvate ferredoxin oxidoreductase (*porAB*) were induced, pointing to potential increases in substrate level phosphorylation and electron flow. In parallel with the increased electron flow, a number of operons encoding redox proteins participating in periplasmic electron transfer were also up-regulated, including that encoding the periplasmic [NiFe] hydrogenase (*hynBA-2*) and its putatively associated tetraheme cytochrome (DVU2524-2526) and one encoding a formate dehydrogenase (DVU2810-2812). Thus the possibility exists that these redox proteins are involved in electron transfer to nitrite or in the turnover of reduced electron carriers allowing a greater rate of substrate oxidation for substrate level phosphorylation. Additionally, the fumarate reductase operon (*frdABC*)

was induced, possibly allowing fumarate to serve as an alternative electron acceptor (Table 1).

Among genes involved in the sulfate reduction pathway, the operon for the triheme cytochrome *c*-containing membrane-bound oxidoreductase (*dsrMKJOP*), which has been implicated as having a role in electron transfer for sulfite reduction (Haveman et al., 2004), was considerably down-regulated in response to nitrite. Two other operons with unknown functions, one encoding the membrane-bound decaheme electron transport complex (*rnfABCDEFG*) and the other for the membrane-bound cytoplasmically-oriented Ech hydrogenase (*echABCD*) were also significantly down-regulated.

Genes with functions in nitrogen metabolism

One important observation in response to nitrite was the down-regulation of multiple genes encoding ATP-binding ABC-transporters for amino acids and polyamines (Table 2). With the sulfate reduction pathway and oxidative phosphorylation being severely hindered (Table 1), the decrease in expression of energy linked transport systems could result from a lower energy level in the cells under nitrite stress. The demand for amino acids could also be slowed as a result of the decrease in protein biosynthetic machinery.

Paradoxically, the glutamine synthetase gene (DVU3392), which participates in nitrogen assimilation (Merrick and Edwards, 1995), was induced during nitrite stress (Table 2). This might result from the increased flux of carbon needed to support substrate level phosphorylation that may spill over increasing the ratio of α-ketoglutarate to glutamine, the signal for nitrogen limitation. Additionally, genes encoding the aspartate ammonia-lyase (DVU1766) and asparaginase (DVU2242), which are responsible for the

catabolism of amino acids acquired from the medium, were down-regulated (Table 2). Thus, the transition from respiration of sulfate to alternative energy sources appeared to influence overall carbon and nitrogen metabolism of the cells.

Genes in the predicted Fur regulon

Among the highly induced genes during nitrite stress are ferrous iron transporter genes (Fig. 6), which were predicted to be controlled by the ferric uptake regulator (Fur) at the transcriptional level (Rodionov *et al*., 2004). Interestingly, all genes in the predicted Fur regulon (Rodionov *et al*., 2004) were highly up-regulated for 1.5 hours following the onset of nitrite stress (Table 3). Since the Fur regulons of many bacteria are known to be derepressed by iron deficiency (Escolar *et al*., 1999; Hantke, 2001), its induction in nitrite stress implies a link between this stress and iron depletion. Indeed, genes encoding iron-containing proteins, including nitrite reductase, were on average up-regulated in response to nitrite (Fig. 7), resulting in a higher demand for iron. It is thus likely that the highly induced Fur-regulated genes, which include ferrous iron transporters, served to meet the increased demand for iron.

Genes belonging to the predicted PerR regulon

Because reactive nitrogen species have been shown to trigger oxidative stress responses (Nunoshiba *et al*., 1993; Mukhopadhyay *et al*., 2004), expression levels of genes predicted to be regulated by the oxidative stress regulator PerR (Rodionov *et al*., 2004) were examined (Table 4). All genes in the PerR regulon were moderately up-regulated at

one or more sampling points during the experiment, suggesting oxidative stress response as a derivative from nitrite stress.

Discussion

The sulfate-reducing bacteria are of great potential in the bioremediation of heavy metals and radionuclides in anaerobic environments (White *et al*., 1997; and de Lorenzo, 2002). Therefore, considerable research effort has been made to understand the response of these bacteria to unfavorable environmental factors using physiological and genetic approaches. One significant finding is the inhibition of sulfate reduction by nitrite, an important intermediate during microbial nitrate reduction (Pereira *et al*., 2000; Nemati *et al*., 2001; Haveman *et al*., 2004; Hubert *et al*., 2005). The availability of the genome sequence of *D. vulgaris* makes it possible to study stresses at the whole-genome level (Heidelberg *et al*., 2004). Using global transcriptional analysis, this work revealed that *D. vulgaris* cells responded to the presence of nitrite with a series of well coordinated regulatory pathways linking energy metabolism, nitrogen metabolism, iron homeostasis, and oxidative stress response.

Physiological and transcriptional analyses demonstrated that nitrite reduction was the primary mechanism for detoxification by *D. vulgaris* (Fig. 2 and Table 2), which is consistent with previous observations (Greene *et al*., 2003). A significant increase in the expression of the nitrite reductase genes reported here (Table 2) was also seen by Haveman *et al*. (2004). However, earlier reports measuring the specific activity of nitrite reductase indicated that the enzyme was essentially constitutive (Mitchell *et al*., 1986) or

that activity was actually less in cells exposed to nitrite (Pereira *et al*., 2000). This disparity has not yet been resolved here and requires further examination.

Major effects on energy generation were expected from the biochemical studies that demonstrated nitrite inhibition of sulfite reductase (Wolfe *et al*., 1994; Haveman *et al*., 2004) and the periplasmic [Fe] hydrogenase of *D. vulgaris* (Pereira *et al*., 2000). Furthermore, as nitrite reduction consumes electrons and protons, which are central to respiration, one would expect changes in energy metabolism. Indeed, a number of genes with important roles in energy metabolism were differentially expressed, highlighting the extensive energetic consequences of nitrite stress (Table 1), that are illustrated in the proposed conceptual model of the energetics of nitrite reduction (Fig. 8). *D. vulgaris* cells could respond to this energy requirement by the up-regulation of *ldh* and *porAB*, thus increasing the electron flow and the opportunity for substrate level phosphorylation. Simultaneously, the triheme cytochrome *c* (*dsrMKJOP*) operon, which has been suggested to transfer electrons to the sulfite reductase (Haveman *et al*., 2004), was significantly down-regulated. These results are in good agreement with the earlier work of Haveman *et al*. (2004) who showed repressive effects of nitrite on sulfate reduction including sulfate adenylyl transferase and pyrophosphatase. The outcome of these regulatory events is a redirected electron flow with at least a portion being used for nitrite reduction.

Interestingly, earlier work on the effects of nitrite on the growth of *D. vulgaris* on lactate/sulfate containing medium reported a large accumulation of hydrogen (Pereira *et al*., 2000). Thus some of the excess reductant may be channeled to hydrogen production, although isozyme-2 of the [NiFe] hydrogenase was observed to be up-regulated in our

work. Additionally, the up-regulation of the genes in the fumarate reductase operon (*frdBAC*) (Table 1) could signal the use of fumarate as a terminal electron acceptor in the absence of sulfate/sulfite reduction. Taken as a whole, the repression of sulfate reduction, the increase in nitrite reduction, and the inhibition of [Fe] hydrogenase likely contribute to a diminished proton motive force, which in turn may be responsible for the repression of genes encoding the ATP synthase subunits (Table 1). The resulting slow down in growth might also explain the down-regulation of genes for ribosomal proteins and those for biosynthesis of expensive amino acids during nitrite stress (Fig. 6).

Notably, while the [NiFe] hydrogenase was up-regulated under nitrite stress, the [Fe] hydrogenase was down-regulated (Table 1). Currently, the physiological roles of the various hydrogenases in *D. vulgaris* are still not clear. However, the [NiFe] hydrogenase is apparently more suited to functioning in the presence of nitrite, based on prior reports that nitrite strongly inhibits the periplasmic [Fe] hydrogenase but has no impact on [NiFe] hydrogenase (Berlier *et al*., 1987). Thus, the redundancy in periplasmic hydrogenases may allow for functional compensation under stressconditions (Heidelberg *et al*., 2004).

Furthermore, the up-regulation of periplasmic formate dehydrogenase points to the possibility that formate oxidation acts as another mechanism to supply electrons and protons for nitrite reduction, but the source of formate in the periplasm needs to be resolved. Interestingly, it is proposed that the "hydrogen cycling' model (Odom and Peck, 1981) for contributing to a proton gradient could potentially be one example of a more general phenomenon termed redox cycling (Jormakka *et al*., 2003). In fact, consideration of the *D. vulgaris* genome sequence reveals the potential for production of

formate in the cytoplasm. Movement of the protonated, uncharged species through the cytoplasmic membrane and its oxidation in the periplasm could contribute to the electron and proton flows across the membrane (Heidelberg *et al*., 2004). Thus, it is possible that uncharged formate generated during pyruvate oxidation diffuses across the membrane and then is oxidized by the formate dehydrogenase to contribute to the electrons and protons used in nitrite reduction or hydrogen generation.

The energetic consequences of nitrite stress also affected nitrogen metabolism in *D. vulgaris* (Table 2). The down-regulation of multiple genes encoding ATP-requiring ABC amino acid and polyamine transporters may reflect the inhibition of ATP generation from sulfate respiration and/or the decreased demand for amino acids for protein biosynthesis. In contrast, the up-regulation of the glutamine synthetase gene (*glnA*) would appear to signal nitrogen-limiting conditions (Woods and Reid, 1993; Merrick and Edwards, 1995). It is possible that an increased flux of carbon to support substrate level phosphorylation might overflow into the TCA cycle, altering the α -ketoglutarate/glutamine ratio controlling *glnA* expression. Another strategy to preserve amino acids for biosynthetic demand was the repression of genes encoding aspartate ammonia-lyase and asparaginase, which catabolize amino acids when they are present in excess. Thus the presence of nitrite adversely impacted energy generation and indirectly affected the nitrogen signals of the cells.

Interestingly, results from this study show that genes in the Fur regulon were among the most highly up-regulated genes in response to nitrite stress (Table 3). As Fur is known as the primary regulator of iron homeostasis in many other microorganisms (McHugh *et al*., 2003; Moore and Helmann, 2005), this observation raises a question

about the connection between nitrite stress and iron homeostasis. The Fur family of metallo-regulatory proteins are typically dimeric DNA-binding transcriptional factors that also bind Fe^{2+} as co-repressor in order to repress downstream genes. Therefore, derepression of Fur regulated genes could be attributed to interactions of nitrite, directly or indirectly, with either the Fur protein, Fe^{2+}, or both. Derepression of the Fur regulon could be effected by iron deficiency resulting from consumption of cytoplasmic Fe(II), since genes encoding many iron-containing proteins, including the nitrite reductase, were up-regulated in response to nitrite. Compounding this demand for iron, chemical oxidation of Fe^{2+} by NO_2^- has been readily observed (Obuekwe *et al*., 1981; Brons *et al*., 1991) and Fe^{3+} is generally unavailable for biosynthesis or signaling. A less likely mechanism posits that nitrite might react directly with the protein-bound Fe^{2+} co-repressor, generating Fe^{3+}, leading to dissociation and concomitant derepression. The intracellular concentrations of NO_2^- are likely to be small because of the rapid reduction of nitrite in the periplasm and the apparent absence of a specific transport system for this ion. However, given the complex chemistry of reactive nitrogen species (Poole, 2005), it is still possible that reactive nitrogen species generated from nitrite reduction could enter the cytoplasm to react with Fe^{2+} (D'Autréaux *et al*., 2002). However, the contribution of each mechanism to the relief from Fur repression during nitrite exposure is not clear and further biochemical study is needed to address the mechanism and importance of Fur regulation in this stress response in *D. vulgaris*.

Since Fur and PerR both respond to oxidative stress and belong to the same superfamily of metalloregulatory proteins that respond to metal ions (Mongkolsuk and Helmann, 2002), it is possible that the same mechanism derepresses both regulons.

Studies on other microorganisms have shown that reactive nitrogen species, including nitrite, incidentally induce genes responsive to oxidative stress, in addition to genes specifically designed to protect cells from nitrosative stress (Moore *et al*., 2004; Mukhopadhyay *et al*., 2004). Whether proteins encoded in the PerR regulon confer protection against nitrite or are adventitiously derepressed remains to be determined.

In summary, the results reveal that *D. vulgaris* cells initiate a coordination of transcriptional regulations allowing the alleviation of nitrite toxicity via nitrite reduction. The inhibition of energy metabolism pathways could force *D. vulgaris* to shift the flow of reducing equivalents from oxidative phosphorylation to nitrite reduction. In addition, substrate level phosphorylation becomes prominent and the excess reductant generated may be disposed of as succinate or hydrogen. Increased demand for iron resulting from these regulatory events likely contributes to iron depletion along with the chemical oxidation of available Fe^{2+}, derepressing the Fur regulon. However, further biochemical study is needed to elucidate the regulatory mechanisms and importance of transcriptional regulators in *D. vulgaris* during stress responses.

Experimental procedures

Organism and growth conditions

Desulfovibrio vulgaris strain Hildenborough (ATCC 29579) was grown in an anaerobic medium containing lactate plus sulfate (LS medium) of the following composition (per liter): 6.72 g of sodium lactate, 7.10 g of Na_2SO_4, 0.963g of anhydrous $MgSO_4$, 1.07 g of NH_4Cl, 0.383 g of K_2HPO_4, 0.088 g of $CaCl_2 \cdot 2H_2O$, 0.620 mg of resazurin, 0.600 g of

Na_2CO_3, 25.0 ml of 1 M HEPES (4-(2-hydroxyethyl)-1-piperazineethanesulfonic acid) (pH 7.0), 12.5 ml of a trace mineral solution, 0.75 g of L-cysteine, and 1.0 g of yeast extract. The trace mineral solution contained the following (per liter): 1.0 g of $FeCl_2 \cdot 4H_2O$, 0.3 g of $CoCl_2 \cdot 4H_2O$, 0.5 g of $MnCl_2 \cdot 4H_2O$, 0.2 g of $ZnCl_2$, 20 mg of H_3BO_3, 50 mg of $Na_2MoO_4 \cdot 4H_2O$, and 0.1 g of $NiCl_2 \cdot 6H_2O$. Cysteine was added as a reductant after the medium had been boiled and cooled to room temperature. The headspace of the medium container was continuously flushed with oxygen-free nitrogen gas, and the pH was adjusted to 7.2±0.1 with 5 M NaOH. A vitamin solution (10ml per liter) (Brandis and Thauer, 1981) was added to the autoclaved medium from filter-sterilized anaerobic stock solutions. Cultures were incubated in the dark at 37°C in stoppered 160-ml serum bottles with 100 ml of LS medium or in 30-ml anaerobic culture tubes with 10 ml of medium and sealed with butyl rubber stoppers and aluminum seals. Strictly anaerobic techniques were used throughout all experimental manipulations.

Oligonucleotide probe design and microarray construction

DNA microarrays covering 3,482 of the 3,531 annotated protein-coding sequences of the *D. vulgaris* genome were constructed with 70mer oligonucleotide probes (He *et al*., 2005). Oligonucleotide probes (3,574) were designed to cover all open read frames (ORFs) for the genome of *D. vulgaris* Hildenborough using a computer software tool ArrayOligoSelector (Bozdech *et al*., 2003) based on an early version (June 2003) of the gene model with 3,584 ORFs. The specificity of all designed oligonucleotide probes was examined with two criteria. From a BLAST analysis (Altschul *et al*., 1997), oligonucleotides (496) were considered non-specific if they showed a >85% sequence

identity or a >18-base continuous homologous stretch with other ORFs in the genome (He *et al*., 2005). These non-specific oligonucleotide probes were re-designed against the genome using two other programs, OligoPicker (Wang and Seed, 2003) and OligoArray (Rouillard *et al*., 2002) with the same design parameters. Following the examination of the entire probe set according to the oligonucleotide probe design criteria (He et al., 2005), 3,471 (97.1%) specific oligonucleotide probes were obtained, and 103 (2.9%) remained non-specific. Ten ORFs with multiple copies had only one probe designed. When this early version gene model was mapped to the published version of the *D. vulgaris* gene model (Heidelberg *et al*., 2004), 3,482 of the 3,531 protein-coding sequences were covered with 3,439 specific, and 43 non-specific oligonucleotide probes.

In addition, 10 oligonucleotides for 10 human genes and 10 oligonucleotides for 10 *Arabidopsis* genes were selected against the *D. vulgaris* genome for positive (with mRNA spiked) or negative (without mRNA spiked) controls. All designed oligonucleotides were commercially synthesized without modification by MWG Biotech Inc., (High Point, NC). The concentration of oligonucleotides was adjusted to 100 pmol/µl. Oligonucleotide probes were prepared in 50% vol/vol DMSO (Sigma-Aldrich, St. Louis, MO) and spotted onto UltraGAPS glass slides (Corning Life Sciences, Corning, NY) using a BioRobotics Microgrid II microarrayer (Genomic Solutions, Ann Arbor, MI). Each oligonucleotide probe had two replicates on a single slide. Additionally, 6 different concentrations (5, 25, 50, 100, 200, and 300 ng/µl) of genomic DNA were also spotted (8 duplicates on a single slide) as additional positive controls. After printing, the oligonucleotide probes were fixed onto the slides by UV cross-linking

(600 mJ of energy) according to the protocol of the manufacturer of the UltraGAPS glass slides (Corning Life Science, Corning. NY).

Exposure to nitrite stress

In experiments for nitrite stress microarray analysis, *D. vulgaris* cultures were grown to exponential phase ($OD_{600\ nm}$ ca. 0.4) in LS medium. To triplicate cultures, nitrite from anaerobic stock solutions was added to a final concentration of 2.5 mM. Cell samples of each culture were harvested immediately after the addition of nitrite (T0), and after 30 (T1), 60 (T2), 90 (T3), 150 (T4), and 240 (T5) min by centrifugation (5,000 × g) for 5 min at 4°C. Cell samples from triplicate control cultures without the addition of nitrite were collected simultaneously at the same time points. Cell pellets were then immediately frozen in liquid N_2 and stored at -80°C prior to RNA isolation. To prevent organic contamination, all glassware was acid washed and baked at 300°C overnight.

Analytical methods

Growth of cultures was monitored spectrophotometrically ($OD_{600\ nm}$). Nitrite and other oxyanions were analyzed on a Dionex DX-120 ion chromatograph (IC) apparatus with a PeakNet analysis software package and a Dionex IonPak Anion Exchange column as previously described (He and Mankin, 2002). The mobile phase contained 1.8 mM Na_2CO_3 and 1.7 mM $NaHCO_3$. Peaks were quantified via an electrochemical detector as conductivity and concentrations were determined using known standards. Samples from the cultures were filtered through 0.20-μm pore-sized filters prior to IC analysis.

Total RNA extraction, purification and labeling

Total cellular RNA was isolated using TRIzol Reagent (Invitrogen, Carlsbad, CA) following the manufacturer's protocol. RNA extracts were purified according to the RNeasy Mini Kit (Qiagen Valencia, CA) instructions and on-column DNase digestion was performed with the RNase-free DNase Set (Qiagen, Valencia, CA) to remove genomic DNA contamination according to the manufacturer's procedure.

To generate cDNA probes with reverse transcriptase, 10 μg of purified total RNA was used for each labeling reaction using a previously described protocol (Thompson *et al*., 2002). Briefly, random hexamers (Invitrogen) were used for priming and the fluorophor Cy3-dUTP or Cy5-dUTP (Amersham Biosciences, Piscataway, NJ) was used for labeling. After the labeling, RNA was removed by NaOH treatment and cDNA was immediately purified with a Qiagen PCR Mini kit. The efficiency of labeling was routinely monitored by measuring the absorbance at 260 nm (for DNA concentration), 550 nm (for Cy3), or 650 nm (for Cy5). Two samples of each total RNA preparation were labeled, one with Cy3-dUTP and another with Cy5-dUTP for microarray hybridization.

Microarray hybridization, washing and scanning

To hybridize microarray glass slides, the Cy5-dUTP-labeled cDNA probes from one nitrite-treated culture were mixed with the Cy3-dUTP-labeled cDNA probes from one untreated control culture and vice versa (dye swap). As a result, each biological sample was hybridized to two microarray slides. Equal amounts of Cy3- or Cy5-labeled probes were mixed and resuspended in 35-40 μl of hybridization solution that contained 50% (vol/vol) formamide, 5 × saline-sodium citrate (5 × SSC; 1X SSC = 150 mM NaCl, 15

mM sodium citrate, pH 7.0), 0.1% (wt/vol) sodium dodecyl sulfate (SDS), and 0.1 mg herring sperm DNA /ml (Invitrogen). The hybridization solution was incubated at 95-98°C for 5 min, centrifuged to collect condensation, kept at 50°C, and applied onto microarray slides. Hybridization was carried out in hybridization chambers (Corning Life Sciences, Corning, NY) at 45°C overnight (16-20 h). 10 μl of 3 × SSC solution was added to the wells at both ends of the microarray slides to maintain proper chamber humidity and probe hydration around the edges of the cover slip. Microarray slides were washed according to the instructions for spotted oligonucleotide microarrays on UltraGAPS slides by the manufacturer (Corning) in the following steps: twice in a solution containing 2 × SSC and 0.1% (wt/vol) SDS at 42°C at 5-min intervals, twice in a solution containing 0.1 × SSC and 0.1% (wt/vol) SDS at room temperature at 10-min intervals, and twice in 0.1 x SSC at room temperature at 2-min intervals. After being blown dry by a stream of N_2, the slides were scanned for the fluorescence intensity of both the Cy5 and Cy3 fluorophores using the ScanArray Express microarray analysis system (Perkin Elmer, Boston, MA).

Image quantification and data analysis

To determine signal fluorescence intensities for each spot, 16-bit TIFF scanned images were analyzed by application of the software ImaGene version 6.0 (Biodiscovery, Marina Del Rey, Calif.) to quantify spot signal, spot quality, and background fluorescent intensities. Empty spots, poor spots, and negative spots were flagged according to the instruction of the software and removed in subsequent analysis (Gao *et al*., 2004).

The resulting data files were subjected to Lowess intensity-based normalization and further analyzed using GeneSpring version 5.1 (Silicon Genetics, Redwood City, Calif.). To assess the statistical significance of individual data points, the Student *t*-test was used to calculate a *p*-value to test the null hypothesis that the expression level was unchanged. A statistical model incorporating both per gene variance and operon structure was further used to compute the posterior probability that each gene changed its expression level in the direction indicated by its mean value (Price *et al*., 2005). An average linkage hierarchical clustering analysis of the time course transcriptional response to nitrite stress with the Euclidean distance as the similarity metric was performed and visualized with Hierarchical Clustering Explorer Version 3.0 (Seo *et al*., 2004).

Analysis of average expression levels of genes encoding iron-containing proteins

The significance of iron-containing proteins was evaluated by comparing the expression levels of transcripts coding for iron-containing proteins to the average values for all genes in the cell. To estimate absolute transcript levels from ratios we fixed control channel measurements to be equal to average values reported in hybridizations using genomic DNA as a reference under similar conditions in our laboratory. Absolute levels (normalized for total cellular mRNA abundance) in treatment conditions were then computed directly from the observed ratios. To identify genes encoding iron-containing proteins, we examined domain structure as predicted by InterPro version 9 and included all genes with domains annotated as binding iron.

Real-time quantitative reverse-transcription-PCR (RT-PCR) analysis

To independently validate gene expression results from the microarray analysis, eight open reading frames (ORFs) were chosen for analysis using real-time RT-PCR. Primer pairs (in parentheses, forward and reverse) were designed for the following genes to yield products of ~100 bp (Rozen and Skaletsky, 2000): DVU0625 (5′-AGAACCTCTGGCTCGGCTAT, 5′-CGATTGATACGGTCGATGTG); DVU0942 (5′-CATCGCCGTATTTCAGGATT, 5′-GAGATGCCCGCCTACTTTC); DVU1290 (5′-TTTCCGGCTTTCAGTACGTT, 5′-AGACTTGGCCCAATCCACTA); DVU1574 (5′-GGTGGCAAGCTCGAAGTCTA, 5′-GATGTCGAGTTCGGTCAGGT); DVU2247 (5′-TCTATCCGCTGGACTTCACC, 5′-ACACCGATGACCTC GACATT); DVU2543 (5′-ACCTCACCATCTACGCCTTG, 5′-GCTTTGGCCGTGTATTCATC); DVU2571 (5′-GAAGGAGGTCATCGTCTCCA, 5′-GGGGTCGTTCCTGATCTGT); DVU2680 (5′-CTTCATTCCCCTTTTCGACTC, 5′-CCCGCAGAAGTACTCGTAGG).

The RT-PCR analysis was carried out using a previously described protocol (Wan et al., 2004). Briefly, the cDNA template for real-time RT-PCR was synthesized from 5 μg of total RNA using the reverse transcriptase reaction with random hexamer priming (Invitrogen). The quantitative PCR was carried out in an iCycler thermal cycler (Bio-Rad, Hercules, Calif.) that measured the increases in fluorescence resulting from the incorporation of SYBR green dye (Molecular Probes, Eugene, Oreg.) into double-strand DNA. Real-time data acquisition and analysis were performed with the software iCycle 2.3 version B according to the manufacturer's instructions. Standards for each gene of interest were obtained by serial dilutions of PCR amplification product from *D. vulgaris* genomic DNA using the procedure described above but without SYBR green dye. The standards were used to establish a standard curve consisting of seven points serially

diluted from 10^7 to 10^1 copies. Copy numbers of the target gene transcripts were determined by comparison with the standard curves and then gene expression differences between the treatment and control samples were determined.

Acknowledgements

This research was supported by the U.S. Department of Energy under the Genomics:GTL Program through the Virtual Institute of Microbial Stress and Survival (VIMSS; http://vimss.lbl.gov), and Microbial Genome Program, of the Office of Biological and Environmental Research, Office of Science, under Cont# DE-AC02-05CH11231.
Oak Ridge National Laboratory is managed by University of Tennessee-Battelle LLC for the Department of Energy under contract DEAC05-00OR22725.

References

Altschul, S., Madden, T., Schäffer, A., Zhang, J., Miller, W., and Lipman, D. (1997) Gapped BLAST and PSI-BLAST: a new generation of protein database search programs. *Nucleic Acids Res* **25**: 3389-3402.

Berlier, Y., Fauque, G.D., LeGall, J., Choi, E.S., Peck, H.D., Jr, and Lespinat, P.A. (1987) Inhibition studies of three classes of *Desulfovibrio* hydrogenase: Application to the further characterization of the multiple hydrogenases found in *Desulfovibrio vulgaris* hildenborough. *Biochem Biophys Res Commun* **146**: 147-153.

Betlach, M.R., and Tiedje, J.M. (1981) Kinetic explanation for accumulation of nitrite, nitric oxide, and nitrous oxide during bacterial denitrification. *Appl Environ Microbiol* **42**: 1074-1084.

Bozdech, Z., Zhu, J.C., Joachimiak, M.P., Cohen, F.E., Pulliam, B., and DeRisi, J.L. (2003) Expression profiling of the schizont and trophozoite stages of *Plasmodium falciparum* with a long-oligonucleotide microarray. *Genome Biol* **4**: R9.

Brandis, A., and Thauer, R.K. (1981) Growth of *Desulfovibrio* species on hydrogen and sulfate as sole energy source. *J Gen Microbiol* **126**: 249-252.

Brons, H.J., Hagen, W.R., and Zehnder, A.J. (1991) Ferrous iron dependent nitric oxide production in nitrate reducing cultures of *Escherichia coli*. *Arch Microbiol* **155**: 341-347.

Chardin, B., Dolla, A., Chaspoul, F., Fardeau, M.L., Gallice, P., and Bruschi, M. (2002) Bioremediation of chromate: thermodynamic analysis of the effects of Cr(VI) on sulfate-reducing bacteria. *Appl Microbiol Biotechnol* **60**: 352-360.

D'Autréaux, B., Touati, D., Bersch, B., Latour, J.-M., and Michaud-Soret, I. (2002) Direct inhibition by nitric oxide of the transcriptional ferric uptake regulation protein via nitrosylation of the iron. *Proc Natl Acad Sci USA* **99**: 16619-16624.

Davidova, I., Hicks, M.S., Fedorak, P.M., and Suflita, J.M. (2001) The influence of nitrate on microbial processes in oil industry production waters. *J Ind Microbiol Biotechnol* **27**: 80-86.

Escolar, L., Perez-Martin, J., and de Lorenzo, V. (1999) Opening the iron box: transcriptional metalloregulation by the Fur protein. *J Bacteriol* **181**: 6223-6229.

Gadd, G.M., and White, C. (1993) Microbial treatment of metal pollution - a working biotechnology? *Trends Biotechnol* **11**: 353-359.

Gao, H., Wang, Y., Liu, X., Yan, T., Wu, L., Alm, E., et al. (2004) Global transcriptome analysis of the heat shock response of *Shewanella oneidensis*. *J Bacteriol* **186**: 7796-7803.

Greene, E.A., Hubert, C., Nemati, M., Jenneman, G.E., and Voordouw, G. (2003) Nitrite reductase activity of sulphate-reducing bacteria prevents their inhibition by nitrate-reducing, sulphide-oxidizing bacteria. *Environ Microbiol* **5**: 607-617.

Hantke, K. (2001) Iron and metal regulation in bacteria. *Curr Opin Microbiol* **4**: 172-177.

Hao, O.J., Chen, J.M., Huang, L., and Buglass, R.L. (1996) Sulfate-reducing bacteria. *Crit Rev Environ Sci Technol* **26**: 155-187.

Haveman, S.A., Greene, E.A., Stilwell, C.P., Voordouw, J.K., and Voordouw, G. (2004) Physiological and gene expression analysis of inhibition of *Desulfovibrio vulgaris* Hildenborough by nitrite. *J Bacteriol* **186**: 7944-7950.

He, Q., and Mankin, K.R. (2002) Assessing removal kinetics of organic matter in rock-plant filters. *Trans ASAE* **45**: 1771-1778.

He, Z., Wu, L., Li, X., Fields, M.W., and Zhou, J. (2005) Empirical establishment of oligonucleotide probe design criteria. *Appl Environ Microbiol* **71**: 3753-3760.

Heidelberg, J.F., Seshadri, R., Haveman, S.A., Hemme, C.L., Paulsen, I.T., Kolonay, J.F., et al. (2004) The genome sequence of the anaerobic, sulfate-reducing bacterium *Desulfovibrio vulgaris* Hildenborough. *Nature Biotechnol* **22**: 554-559.

Hubert, C., Nemati, M., Jenneman, G. E., Voordouw, G. (2005) Corrosion risk associated with microbial souring control using nitrate or nitrite. *Appl Microbiol Biotechnol* **68**: 272-282.

Jenneman, G.E., McInerney, M.J., and Knapp, R.M. (1986) Effect of nitrate on biogenic sulfide production. *Appl Environ Microbiol* **51**: 1205-1211.

Jormakka, M., Byrne, B., and Iwata, S. (2003) Proton motive force generation by a redox loop mechanism. *FEBS Lett* **545**: 25-30.

Kelso, B.H.L., Smith, R.V., and Laughlin, R.J. (1999) Effects of carbon substrates on nitrite accumulation in freshwater sediments. *Appl Environ Microbiol* **65**: 61-66.

Little, B.J., Ray, R.I., and Pope, R.K. (2000) Relationship between corrosion and the biological sulfur cycle: A review. *Corrosion* **56**: 433-443.

Lloyd, J.R., Ridley, J., Khizniak, T., Lyalikova, N.N., and Macaskie, L.E. (1999) Reduction of technetium by *Desulfovibrio desulfuricans*: biocatalyst characterization and use in a flowthrough bioreactor. *Appl Environ Microbiol* **65**: 2691-2696.

Londry, K.L., and Suflita, J.M. (1999) Use of nitrate to control sulfide generation by sulfate-reducing bacteria associated with oily waste. *J Ind Microbiol Biotechnol* **22**: 582-589.

Lovley, D.R., Roden, E.E., Phillips, E.J.P., and Woodward, J.C. (1993a) Enzymatic iron and uranium reduction by sulfate-reducing bacteria. *Marine Geol* **113**: 41-53.

Lovley, D.R., Widman, P.K., Woodward, J.C., and Phillips, E.J.P. (1993b) Reduction of uranium by cytochrome c_3 of *Desulfovibrio vulgaris*. *Appl Environ. Microbiol* **59**: 3572-3576.

Madigan, M.T., Martinko, J.M., and Parker, J. (2000) *Brock biology of microorganisms*. Upper Saddle River, N.J.: Prentice-Hall.

McHugh, J.P., Rodríguez-Quiñones, F., Abdul-Tehrani, H., Svistunenko, D.A., Poole, R.K., Cooper, C.E., et al. (2003) Global iron-dependent gene regulation in *Escherichia coli*: A new mechanism for iron homeostasis. *J Biol Chem* **278**: 29478-29486.

Merrick, M.J., and Edwards, R.A. (1995) Nitrogen control in bacteria. *Microbiol Rev* **59**: 604-622.

Mitchell, G.J., Jones, J.G., and Cole, J.A. (1986) Distribution and regulation of nitrate and nitrite reduction by *Desulfovibrio* and *Desulfotomaculum* species. *Arch Microbiol* **144**: 35-40.

Mongkolsuk, S., and Helmann, J.D. (2002) Regulation of inducible peroxide stress responses. *Mol Microbiol* **45**: 9-15.

Moore, C.M., and Helmann, J.D. (2005) Metal ion homeostasis in *Bacillus subtilis*. *Curr Opin Microbiol* **8**: 188-195.

Moore, C.M., Nakano, M.M., Wang, T., Ye, R.W., and Helmann, J.D. (2004) Response of *Bacillus subtilis* to nitric oxide and the nitrosating agent sodium nitroprusside. *J Bacteriol* **186**: 4655-4664.

Mukhopadhyay, P., Zheng, M., Bedzyk, L.A., LaRossa, R.A., and Storz, G. (2004) Prominent roles of the NorR and Fur regulators in the *Escherichia coli* transcriptional response to reactive nitrogen species. *Proc Natl Acad Sci USA* **101**: 745-750.

Myhr, S., Lillebo, B.L.P., Sunde, E., Beeder, J., and Torsvik, T. (2002) Inhibition of microbial H_2S production in an oil reservoir model column by nitrate injection. *Appl Microbiol Biotechnol* **58**: 400-408.

Natural and Accelerated Bioremediation Research Program (2003) Bioremediation of metals and radionuclides: what it is and how it works. In *NABIR primer*. Hazen, T.C., Benson, S.M., Metting, F.B., Faison, B., Palmisano, A.C. and McCullough, J. (eds). Lawrence Berkeley National Laboratory, Berkeley, Calif.

Nemati, M., Mazutinec, T.J., Jenneman, G.E., and Voordouw, G. (2001) Control of biogenic H_2S production with nitrite and molybdate. *J Ind Microbiol Biotechnol* **26**: 350-355.

Nunoshiba, T., DeRojas-Walker, T., Wishnok, J.S., Tannenbaum, S.R., and Demple, B. (1993) Activation by nitric oxide of an oxidative-stress response that defends *Escherichia coli* against activated macrophages. *Proc Natl Acad Sci USA* **90**: 9993-9997.

Obuekwe, C.O., Westlake, D.W., and Cook, F.D. (1981) Effect of nitrate on reduction of ferric iron by a bacterium isolated from crude oil. *Can J Microbiol* **27**: 692-697.

Odom, J.M., and Peck, H.D., Jr (1981) Hydrogen cycling as a general mechanism for energy coupling in the sulfate-reducing bacteria, *Desulfovibrio* sp. *FEMS Microbiol Lett* **12**: 47-50.

Pereira, I.A.C., LeGall, J., Xavier, A.V., and Teixeira, M. (2000) Characterization of a heme *c* nitrite reductase from a non-ammonifying microorganism, *Desulfovibrio vulgaris* Hildenborough. *Biochim Biophys Acta* **1481**: 119-130.

Peterson, J.D., Umayam, L.A., Dickinson, T., Hickey, E.K., and White, O. (2001) The comprehensive microbial resource. *Nucleic Acids Res* **29**: 123-125.

Poole, R.K. (2005) Nitric oxide and nitrosative stress tolerance in bacteria. *Biochem Soc Trans* **33**: 176-180.

Postgate, J.R. (1984) *The sulfate-reducing bacteria.* Cambridge, UK: Cambridge University Press.

Price, M.N., Huang, K. H., Alm, E.J., and Arkin, A.P. (2005) A novel method for accurate operon predictions in all sequenced prokaryotes. *Nucleic Acids Res* **33**: 880-892.

Riley, R.G., and Zachara, J. (1992) *Chemical contaminants on DOE lands and selection of contaminant mixtures for subsurface research.* DOE/ER-0547T. U.S. Department of Energy, Washington, D.C.

Rodionov, D.A., Dubchak, I., Arkin, A.P., Alm, E., and Gelfand, M.S. (2004) Reconstruction of regulatory and metabolic pathways in metal-reducing δ -proteobacteria. *Genome Biol* **5**: R90.

Rouillard, J.M., Herbert, C.J., and Zuker, M. (2002) OligoArray: genome-scale oligonucleotide design for microarrays. *Bioinformatics* **18**: 486-487.

Rozen, S., and Skaletsky, H.J. (2000) Primer3 on the WWW for general users and for biologist programmers. In *Bioinformatics methods and protocols: Methods in molecular biology*. Krawetz, S. and Misener, S. (eds). Totowa, N.J.: Humana Press, pp. 365-386.

Seo, J., Bakay, M., Chen, Y.-W., Hilmer, S., Shneiderman, B., and Hoffman, E.P. (2004) Interactively optimizing signal-to-noise ratios in expression profiling: project-specific

algorithm selection and detection *p*-value weighting in Affymetrix microarrays. *Bioinformatics* **20**: 2534-2544.

Singleton, R., Jr. (1993) The sulfate-reducing bacteria: an overview. In *The sulfate-reducing bacteria: contemporary perspectives*. Odom, J.M. and Singleton, R., Jr. (eds). New York, N.Y.: Springer-Verlag, pp. 1-21.

Thompson, D.K., Beliaev, A.S., Giometti, C.S., Tollaksen, S.L., Khare, T., Lies, D.P., et al. (2002) Transcriptional and proteomic analysis of a ferric uptake regulator (fur) mutant of *Shewanella oneidensis*: Possible involvement of fur in energy metabolism, transcriptional regulation, and oxidative stress. *Appl Environ Microbiol* **68**: 881-892.

Valls, M., and de Lorenzo, V. (2002) Exploiting the genetic and biochemical capacities of bacteria for the remediation of heavy metal pollution. *FEMS Microbiol Rev* **26**: 327-338.

van den Berg, W.A.M., Hagen, W.R., and van Dongen, W.M.A.M. (2000) The hybrid-cluster protein (`prismane protein') from *Escherichia coli* - Characterization of the hybrid-cluster protein, redox properties of the [2Fe-2S] and [4Fe-2S-2O] clusters and identification of an associated NADH oxidoreductase containing FAD and [2Fe-2S]. *Eur J Biochem* **267**: 666-676.

van Rijn, J., Tal, Y., and Barak, Y. (1996) Influence of volatile fatty acids on nitrite accumulation by a *Pseudomonas stutzeri* strain isolated from a denitrifying fluidized bed reactor. *Appl Environ Microbiol* **62**: 2615-2620.

Wan, X.-F., VerBerkmoes, N.C., McCue, L.A., Stanek, D., Connelly, H., Hauser, L.J., et al. (2004) Transcriptomic and proteomic characterization of the Fur modulon in the metal-reducing bacterium *Shewanella oneidensis*. *J Bacteriol* **186**: 8385-8400.

Wang, X.W., and Seed, B. (2003) Selection of oligonucleotide probes for protein coding sequences. *Bioinformatics* **19**: 796-802.

White, C., Sayer, J.A., and Gadd, G.M. (1997) Microbial solubilization and immobilization of toxic metals: key biogeochemical processes for treatment of contamination. *FEMS Microbiol Rev* **20**: 503-516.

Wolfe, B.M., Lui, S.M., and Cowan, J.A. (1994) Desulfoviridin, a multimeric-dissimilatory sulfite reductase from *Desulfovibrio vulgaris* (Hildenborough) Purification, characterization, kinetics and EPR studies. *Eur J Biochem* **223**: 79-89.

Wolfe, M.T., Heo, J., Garavelli, J.S., and Ludden, P.W. (2002) Hydroxylamine reductase activity of the hybrid cluster protein from *Escherichia coli*. *J Bacteriol* **184**: 5898-5902.

Woods, D.R., and Reid, S.J. (1993) Recent developments on the regulation and structure of glutamine synthetase enzymes from selected bacterial groups. *FEMS Microbiol Rev* **11**: 273-284.

Table 1. Effect of nitrite exposure on the transcriptional responses of *Desulfovibrio vulgaris* genes involved in energy metabolism

Gene ID	Annotation	Fold Change (Treatment/Control)[a]				
		0.5h	1.0h	1.5h	2.5h	4.0h
Up-regulation:						
DVU0172	iron-sulfur cluster-binding protein	+3.0	+2.8	+1.8	-2.0	-3.3
DVU0173	thiosulfate reductase, putative	+2.5	+1.9	+1.5	-1.8	-2.2
DVU0600	L-lactate dehydrogenase (Ldh)	+2.1	+1.8	+1.9	-	-
DVU0624	NapC/NirT cytochrome *c* family protein	+13.5	+11.4	+12.2	+9.4	+11.4
DVU0625	cytochrome *c* nitrite reductase, catalytic subunit NfrA, putative	+18.5	+12.8	+14.9	+7.5	+5.7
DVU1080	iron-sulfur cluster-binding protein	+54.2	+81.8	+58.6	+28.7	+27.2
DVU1081	iron-sulfur cluster-binding protein	+12.6	+10.5	+12.5	+6.8	+7.2
DVU1569	pyruvate ferredoxin oxidoreductase, alpha subunit (PorA)	—	+2.0	+2.3	—	—
DVU1570	pyruvate ferredoxin oxidoreductase, beta subunit (PorB)	—	+2.2	+2.3	—	—
DVU2524	cytochrome c_3, putative	+2.2	+3.4	+5.0	—	—
DVU2525	periplasmic [NiFe] hydrogenase, small subunit, isozyme 2 (HynB-2)	—	+1.5	+1.6	—	—
DVU2526	periplasmic [NiFe] hydrogenase, large subunit, isozyme 2 (HynA-2)	+8.1	+9.1	+9.5	+4.7	+3.2
DVU2543	hybrid cluster protein	+27.5	+34.5	+65.1	+82.7	+37.3
DVU2544	iron-sulfur cluster-binding protein	+39.8	+50.7	+82.0	+233	+30.3
DVU2810	formate dehydrogenase formation protein FdhE, putative	+1.5	—	+1.5	+1.8	—
DVU2811	formate dehydrogenase, beta subunit, putative	—	—	+2.1	+2.8	—
DVU2812	formate dehydrogenase, alpha subunit, selenocysteine-containing (FdnG-3)	—	—	+1.8	—	—
DVU3261	fumarate reductase, cytochrome *b* subunit (FrdC)	+2.0	+3.5	+3.2	—	—
DVU3262	fumarate reductase, flavoprotein subunit (FrdA)	+1.8	+2.9	+2.6	—	+1.4
DVU3263	fumarate reductase, iron-sulfur protein (FrdB)	+1.9	+3.7	+3.1	—	—
Down-regulation:						
DVU0431	Ech hydrogenase, subunit EchD, putative	-2.7	-1.9	—	—	—
DVU0432	Ech hydrogenase, subunit EchC, putative	-2.4	-2.0	-1.7	—	—
DVU0433	Ech hydrogenase, subunit EchB, putative	-2.0	-1.7	—	—	—
DVU0434	Ech hydrogenase, subunit EchA, putative	-1.7	-1.7	—	—	—
DVU0774	ATP synthase, F_1 epsilon subunit (AtpC)	—	-2.4	-2.6	-2.2	—
DVU0775	ATP synthase, F_1 beta subunit (AtpD)	—	-3.2	-3.1	-3.4	—
DVU0776	ATP synthase, F_1 gamma subunit (AtpG)	—	-3.3	-2.4	-5.5	—
DVU0777	ATP synthase, F_1 alpha subunit (AtpA)	-2.5	-3.2	-4.4	-4.2	—
DVU0778	ATP synthase, F_1 delta subunit (AtpH)	-2.1	-3.3	-2.6	-4.0	—
DVU0779	ATP synthase F_0, B subunit, putative (AtpF2)	-1.8	-2.6	-2.8	-2.5	—
DVU0780	ATP synthase F_0, B subunit, putative (AtpF1)	-2.3	-2.5	-2.5	—	—
DVU0917	ATP synthase F_0, C subunit (AtpE)	—	-2.7	-3.4	-3.2	-1.7
DVU0918	ATP synthase F_0, A subunit (AtpB)	-2.2	-2.7	-3.5	-2.4	-1.5
DVU1286	reductase, transmembrane subunit, putative (DsrP)	-3.0	-3.0	-4.2	-1.8	—
DVU1287	reductase, iron-sulfur binding subunit, putative (DsrO)	-5.3	-5.3	-6.0	-1.8	—
DVU1288	cytochrome c family protein (DsrJ)	-5.2	-4.8	-4.4	-2.3	—

DVU1289	reductase, iron-sulfur binding subunit, putative (DsrK)	-6.7	-5.1	-4.6	-2.1	—
DVU1290	nitrate reductase, gamma subunit, putative (DsrM)	-6.4	-5.7	-5.9	-1.9	—
DVU1769	periplasmic [Fe] hydrogenase, large subunit (HydA)	—	-1.7	-2.6	—	-2.6
DVU1770	periplasmic [Fe] hydrogenase, small subunit (HydB)	-1.8	-2.4	-4.2	-4.1	-4.8
DVU2792	electron transport complex protein RnfC, putative	-2.3	-3.0	-2.4	-2.1	-2.0
DVU2793	electron transport complex protein RnfD, putative	-1.7	-2.8	-1.7	-2.1	-1.8
DVU2794	electron transport complex protein RnfG, putative	-2.0	-2.8	-2.1	-2.3	-2.0
DVU2795	electron transport complex protein RnfE, putative	—	-2.5	—	-2.1	—
DVU2796	electron transport complex protein RnfA, putative	—	-2.1	-1.7	-1.8	-1.6
DVU2797	iron-sulfur cluster-binding protein	—	-2.4	—	-1.6	—
DVU2798	ApbE family protein	-1.7	-2.4	-1.9	-1.6	—

[a]Changes of gene expression level at different time points following addition of 2.5 mM sodium nitrite to cultures compared to controls without nitrite addition. Expression levels were obtained at the same time points from both the treatment and control cultures for the calculation of the expression fold changes resulting from the stressor. Positive fold change values denote increases in gene expression and negative fold change values indicate decreases in gene expression ($p<0.05$). Dash signs indicate that no significant change in gene expression was observed.

Table 2. Effect of nitrite exposure on the transcriptional responses of *Desulfovibrio vulgaris* genes involved in nitrogen metabolism

Gene ID	TIGR Annotation	Fold Change (Treatment/Control)[a]				
		0.5h	1.0h	1.5h	2.5h	4.0h
DVU0095	polyamine ABC transporter, periplasmic polyamine-binding protein	-4.1	-5.2	-4.7	—	—
DVU0105	glutamine ABC transporter, ATP-binding protein	-3.3	-2.1	-1.7	—	—
DVU0106	glutamine ABC transporter, permease protein	-1.6	-1.6	-1.6	—	—
DVU0107	glutamine ABC transporter, periplasmic glutamine-binding protein	-2.5	-3.4	-2.5	—	—
DVU0388	amino acid ABC transporter, ATP-binding protein	-4.0	-5.2	-3.6	—	—
DVU0624	NapC/NirT cytochrome *c* family protein	+13.5	+11.4	+12.2	+9.4	+11.4
DVU0625	cytochrome *c* nitrite reductase, catalytic subunit NfrA, putative	+18.5	+12.8	+14.9	+7.5	+5.7
DVU0751	amino acid ABC transporter, permease protein, His/Glu/Gln/Arg/opine family	-2.0	-2.5	-2.4	-1.9	-2.2
DVU0752	amino acid ABC transporter, amino acid-binding protein	-2.1	-3.9	-3.0	-3.6	-3.8
DVU0966	amino acid ABC transporter, periplasmic amino acid-binding protein	-2.5	-5.9	-5.8	-2.6	-3.8
DVU0967	amino acid ABC transporter, permease protein, His/Glu/Gln/Arg/opine family	-2.1	-2.5	-1.8	—	—
DVU0968	amino acid ABC transporter, ATP-binding protein	-3.1	-2.6	-2.8	—	—
DVU1026	uracil permease	-7.0	-4.7	-3.4	—	-2.1
DVU1237	amino acid ABC transporter, permease protein, His/Glu/Gln/Arg/opine family	-3.6	-1.6	-2.4	—	—
DVU1238	amino acid ABC transporter, periplasmic amino acid-binding protein	-2.6	-1.6	-3.1	—	-2.1
DVU1766	aspartate ammonia-lyase, putative	-1.9	-2.1	-2.8	-2.0	-1.9
DVU2113	xanthine/uracil permease family protein	-4.3	-3.6	-3.2	—	-1.9
DVU2242	asparaginase family protein	-1.6	-1.7	-2.0	—	—
DVU2543	hybrid cluster protein	+27.5	+34.5	+65.1	+82.7	+37.3
DVU3392	glutamine synthetase, type I	+1.5	+2.2	+2.8	+2.2	+1.6

[a]Changes of gene expression levels in treatment cultures exposed to 2.5 mM nitrite compared to controls without nitrite addition. Expression levels were obtained at the same time points from both the treatment and control cultures for the calculation of fold changes in expression resulting from the stressor. Positive fold change values denote increase in gene expression and negative fold change values indicate decreases in gene expression ($p<0.05$). Dashes indicate that no significant change in gene expression was observed.

Table 3. Effect of nitrite exposure on the transcriptional responses of *Desulfovibrio vulgaris* genes in the predicted Fur regulon[a]

Gene ID	TIGR Annotation	Fold Change (Treatment/Control)[b]				
		0.5h	1.0h	1.5h	2.5h	4.0h
DVU0763	GGDEF domain protein	+11.9	+2.1	—	—	—
DVU2378	transcriptional regulator, AraC family	+4.3	+4.1	+2.4	—	—
DVU2574	ferrous iron transport protein, putative FeoA	+3.5	+5.0	+3.9	—	—
DVU2680	Flavodoxin	+27.6	+22.6	+4.9	—	—
DVU3330	conserved hypothetical protein	+2.3	+5.7	+2.3	—	—
DVU0273	conserved hypothetical protein	+15.3	+5.2	+1.8	—	-2.2
DVU0304	hypothetical protein	+34.0	+10.1	+3.7	—	—

[a]Predicted Fur-binding sites from Rodionov *et al*. (2004).

[b]Changes in gene expression levels following addition of 2.5 mM sodium nitrite to treatment cultures compared to controls without nitrite addition. Expression levels were obtained at the same time points from both the treatment and control cultures for the calculation of expression fold changes resulting from the stressor. Positive fold change values denote increases in gene expression level and negative fold change values indicate decreases in gene expression level ($p<0.05$). Dashes indicate that no significant change in gene expression was observed.

Table 4. Effect of nitrite exposure on the transcriptional responses of *Desulfovibrio vulgaris* genes in the predicted PerR regulon[a]

Gene ID	TIGR Annotation	Fold Change (Treatment/Control)[b]				
		0.5h	1.0h	1.5h	2.5h	4.0h
DVU0772	hypothetical protein	+1.8	+2.4	+2.6	+2.1	—
DVU2247	antioxidant, AhpC/Tsa family	+3.0	+3.1	+2.1	+1.8	—
DVU2318	rubrerythrin, putative	—	—	+1.5	—	-1.9
DVU3095	Transcriptional regulator, Fur family, PerR	—	—	—	+2.2	—
DVU3096	hypothetical protein	—	+1.8	—	—	—

[a]Predicted PerR-binding sites from Rodionov *et al*. (2004).

[b]Changes of gene expression levels following addition of 2.5 mM sodium nitrite to treatment cultures compared to controls without nitrite addition. Expression levels were obtained at the same time point from both the treatment and control cultures for the calculation of expression fold changes resulting from the stressor. Positive fold change values denote increases in gene expression level and negative fold change values indicate decreases in gene expression level ($p<0.05$). Dashes indicate that no significant change in gene expression was observed.

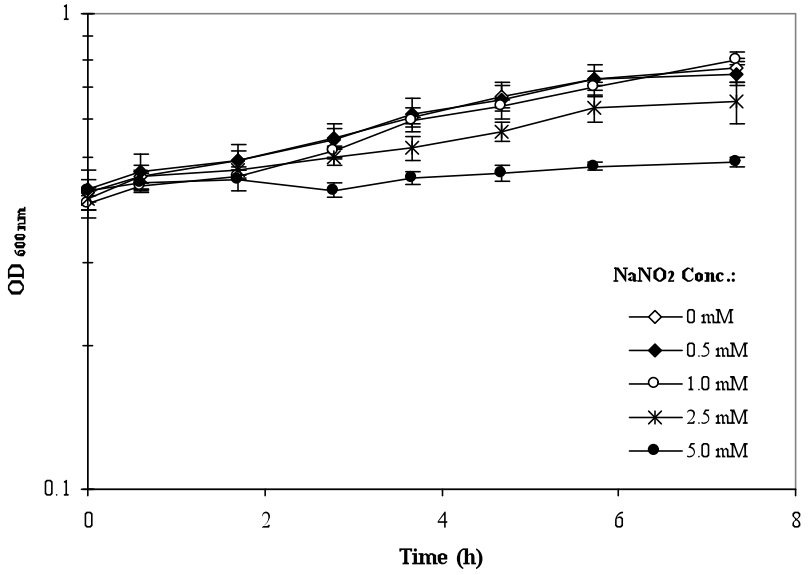

Fig. 1. Impact of nitrite on the growth of *D. vulgaris*. Nitrite of different concentrations was added to sulfate-reducing bacterial cultures in mid-log phase and growth was subsequently monitored as $OD_{600\ nm}$. Data are averaged from triplicate cultures with error bars indicating standard deviations.

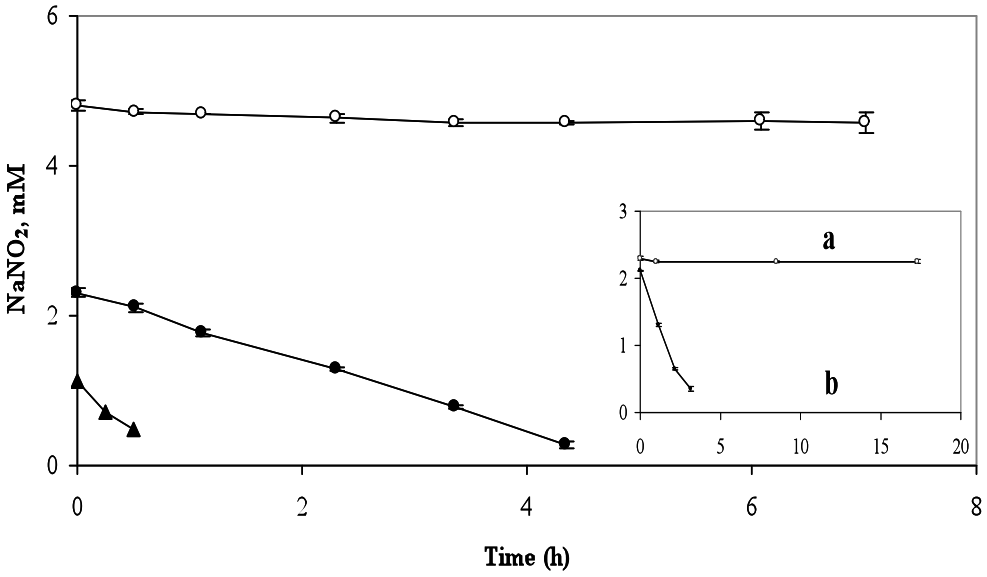

Fig. 2. Changes in sodium nitrite concentrations in *D. vulgaris* cultures. Following the addition of various concentrations of nitrite into mid-log-phase cultures ($OD_{600\ nm}$, 0.4), reduction of nitrite was monitored over time. The inset shows the changes in nitrite concentration in the presence of (a) 40 mM sulfide but no cells or (b) mid-log cells ($OD_{600\ nm}$, 0.4) with sulfide present in the growth medium. Results shown are averages of triplicates with error bars indicating standard deviation.

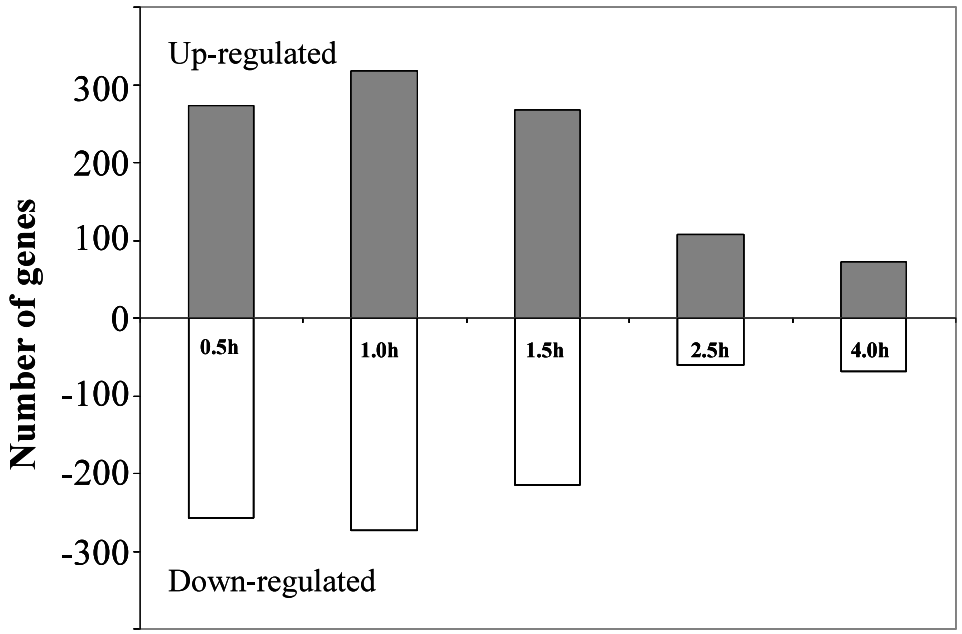

Fig. 3. Temporal profiling of the transcriptional response to sodium nitrite by *Desulfovibrio vulgaris*. Each column represents the number of genes showing significant changes (p<0.05) in gene expression level versus time elapsed following addition of nitrite. Positive and negative values indicate up-and down-regulation, respectively.

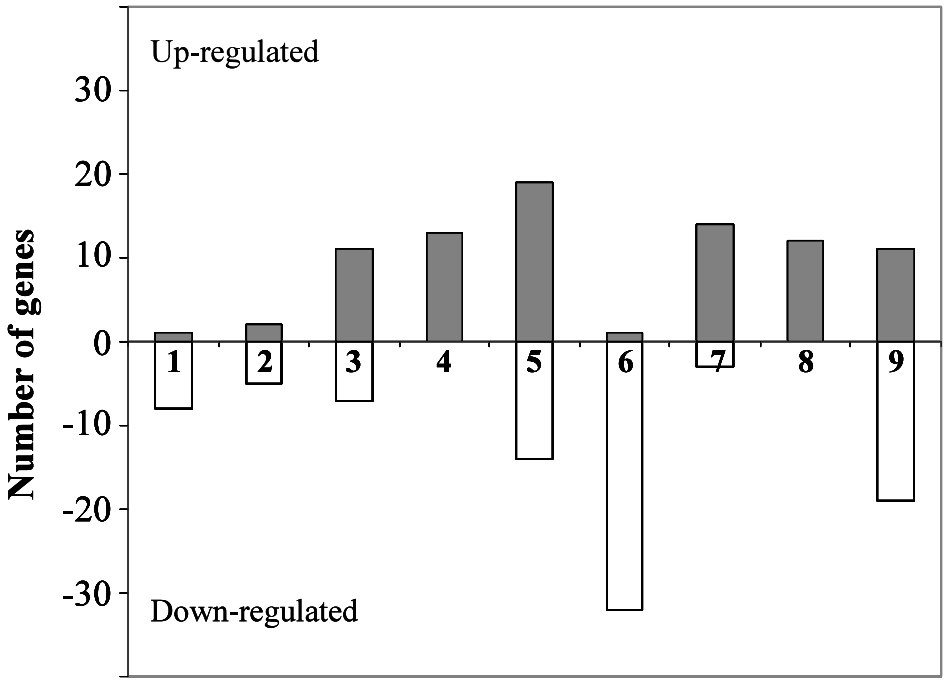

Fig. 4. Functional profiling of the transcriptional response by *Desulfovibrio vulgaris* 1 h following 2.5 mM sodium nitrite addition. The functional role category annotation is that provided by the Institute of Genomic Research (TIGR—www.tigr.org). Each column represents the number of genes in a selected functional category showing significant changes in mRNA abundance in response to nitrite. Positive and negative values indicate up-and down-regulation, respectively. Columns: 1, amino acid biosynthesis; 2, biosynthesis of cofactors, prosthetic groups, and carriers; 3, cell envelope; 4, cellular processes; 5, energy metabolism; 6, protein synthesis; 7, regulatory functions; 8, signal transduction; and 9, transport and binding proteins. Shown are selected role categories with highly differentially expressed genes (fold>3).

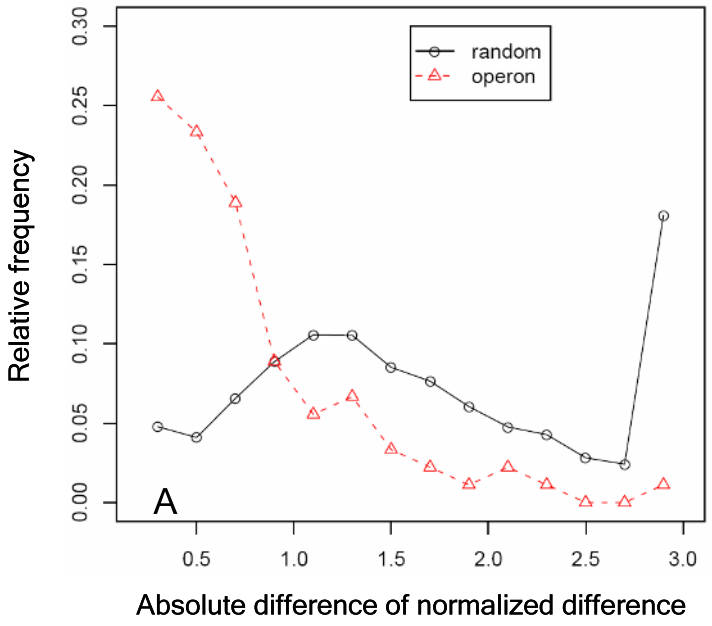

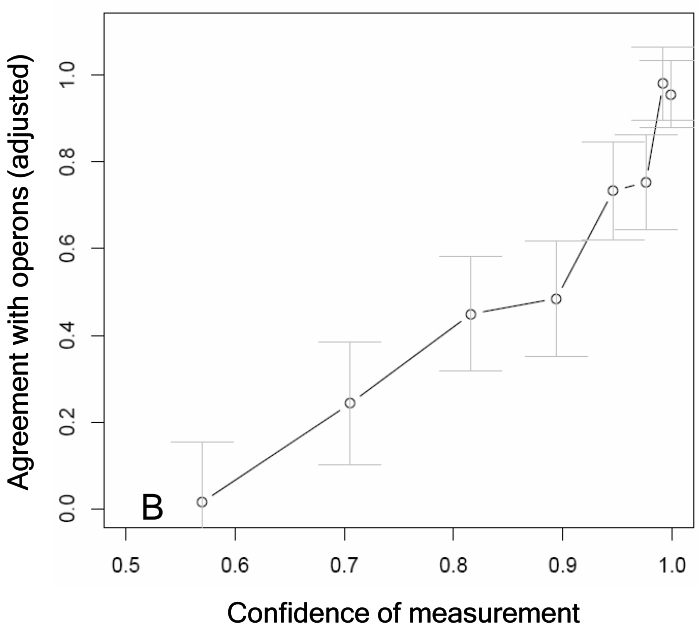

Fig. 5. Validation of microarray results by computational approaches. (A) Log ratio expression difference of gene pairs within the same operon versus gene pairs selected at random. The normalized frequency was plotted against the ratio expression difference

between the treatments and control. Genes within the same operon responded more similarly than genes randomly selected from the genome under sodium nitrite exposure. (B) Agreement within predicted operons at the 90min time point. All genes were divided into eight groups based on the confidence level of the measured change computed by the OpWise program. A confidence of 0.5 indicates complete uncertainty as to whether the gene was up- or down-regulated, while a value of 1 indicates certainty that the measured change in mean reflects the actual direction of change. The y-axis shows the fraction of genes (above that expected by chance) in each group that changed in the same direction as adjacent genes predicted to be in the same operon, together with 95% confidence intervals for the estimate. Values near 1 indicate perfect agreement with all co-operonic genes changing in the same direction, while values near 0 indicate the level of agreement expected by chance (i.e. 50%).

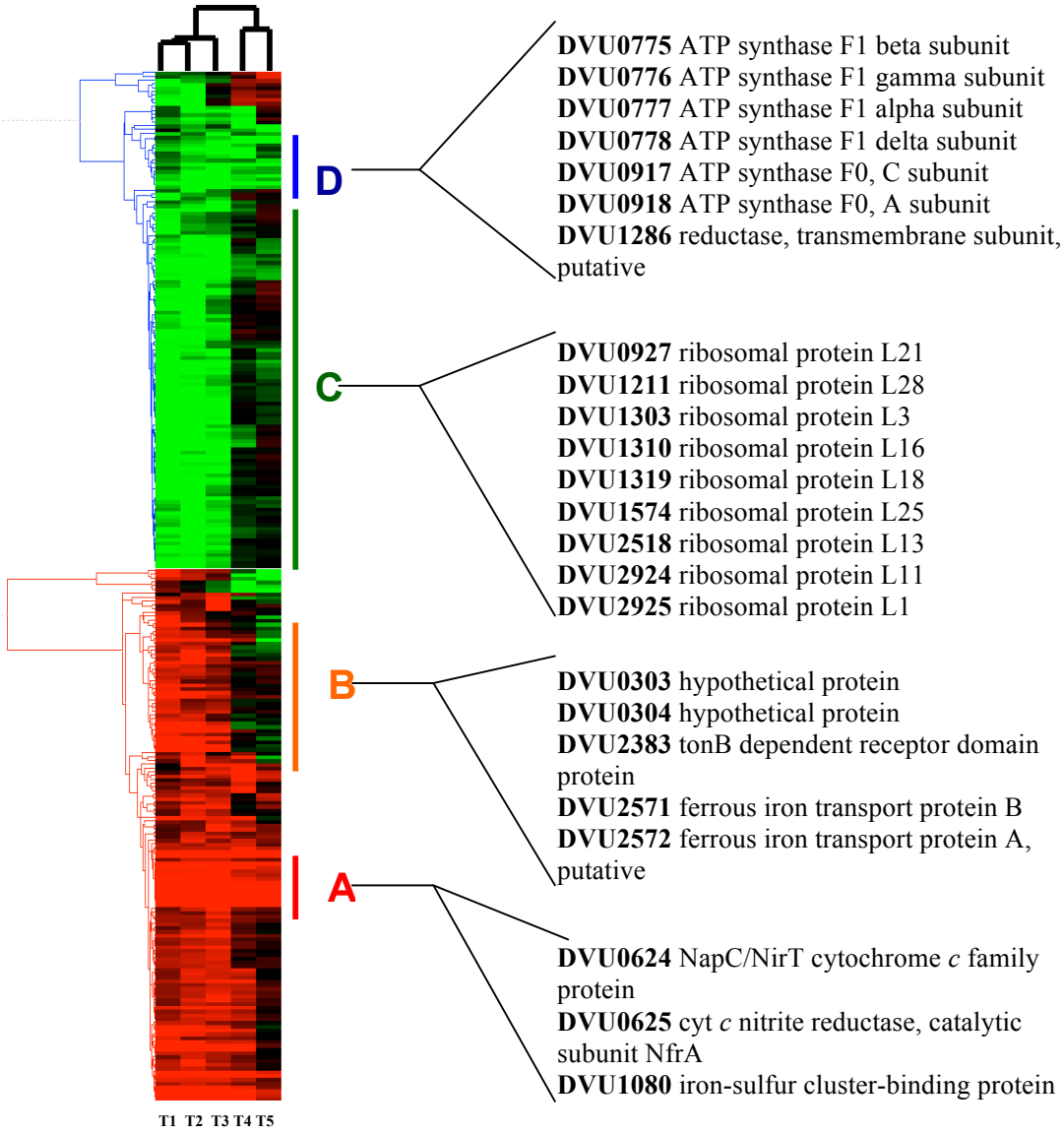

Fig. 6. Hierarchical clustering of selected genes with significant changes (P <0.05 and a fold change of >2 at least at one time point) in expression in response to 2.5 mM nitrite. The red color indicates up-regulation, whereas the green color represents repression. Each row represents the expression of a single gene and each column represents an individual time point following nitrite addition: T1, 0.5 h; T2, 1.0 h; T3, 1.5 h; T4, 2.5 h; T5, 4.0 h. Listed genes are examples from each cluster. Cluster A consists of genes highly induced throughout the duration of the experiment; Cluster B, genes highly induced within 1.5 hour of the addition of nitrite but the induction diminished or even reversed subsequently; Cluster C, genes repressed during the early response to nitrite but the repression was later alleviated; and Cluster D, genes down-regulated throughout the experiment.

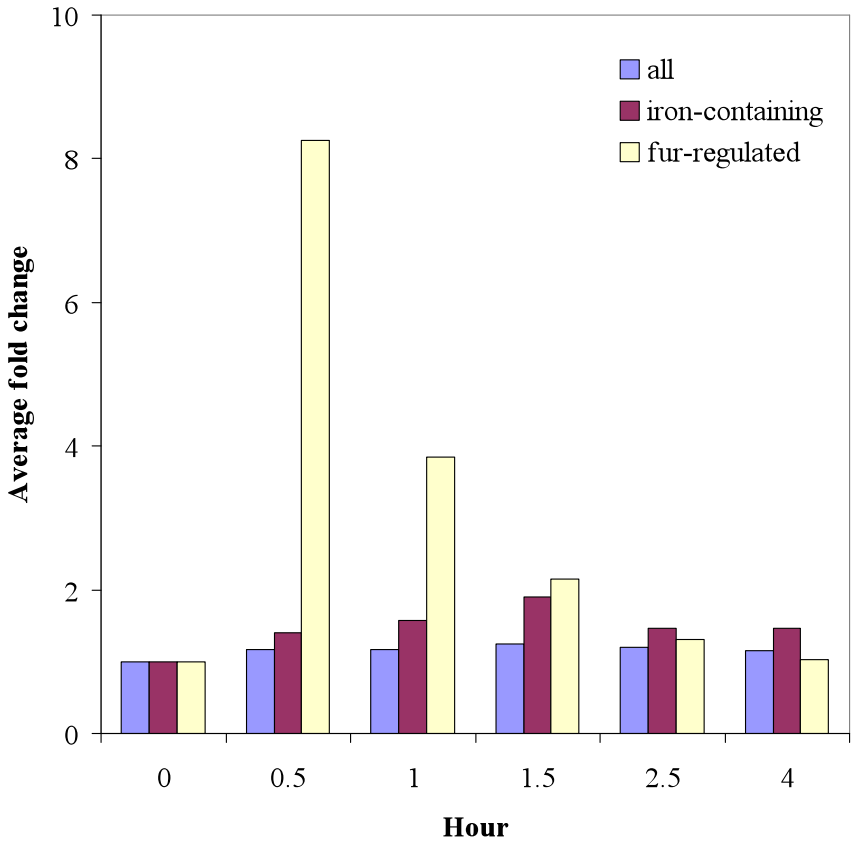

Fig. 7. Average changes in expression level of selected *Desulfovibrio vulgaris* gene groups following 2.5 mM sodium nitrite addition. Blue, all genes covered by the microarray; burgundy, genes encoding iron-containing proteins; and pale yellow, genes belonging to the predicted Fur-regulon (Rodionov *et al*., 2004).

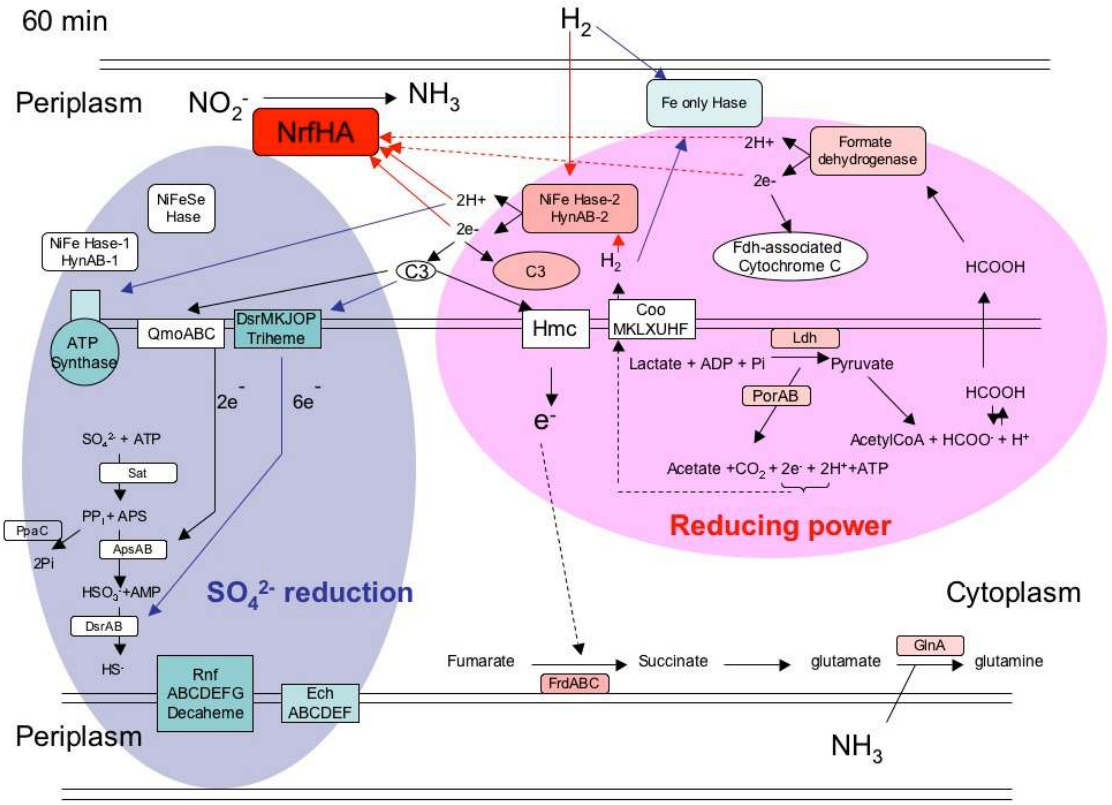

Fig. 8. Conceptual model of the energy pathways responding to nitrite stress (2.5 mM $NaNO_2$) by *Desulfovibrio vulgaris* based on the transcriptional profile obtained 60 min after stress exposure. With the inhibition of the *dsrMKJOP* triheme transmembrane complex by nitrite, reducing equivalents derived from lactate oxidation were shifted to nitrite reduction. Color code: red designates up-regulation and blue designates down-regulation; changes in the intensity of the red or blue color represent the extent of the up- or down regulation, respectively; white color indicates no change detected in expression level.